



**Bulk Crystal Growth of Hybrid Perovskite Material  
CH<sub>3</sub>NH<sub>3</sub>PbI<sub>3</sub>**

Journal:	<i>CrystEngComm</i>
Manuscript ID:	CE-ART-10-2014-002106.R1
Article Type:	Paper
Date Submitted by the Author:	09-Nov-2014
Complete List of Authors:	Tao, Xutang; Shandong University, State Key Laboratory of Crystal Materials Dang, Yangang; Shandong University, State Key Laboratory of Crystal Materials Liu, Yang; Shandong University, State Key Laboratory of Crystal Materials sun, youxuan; Shandong University, State Key Laboratory of Crystal Materials Yuan, Dongsheng; Shandong University, State Key Laboratory of Crystal Materials Liu, Xiaolong; Shandong University, State Key Laboratory of Crystal Materials Lu, Weiqun; Shandong University, State Key Laboratory of Crystal Materials Liu, Guangfeng; Shandong University, Xia, Haibing; Shandong University, State Key Laboratory of Crystal Materials

## Bulk Crystal Growth of Hybrid Perovskite Material $\text{CH}_3\text{NH}_3\text{PbI}_3$

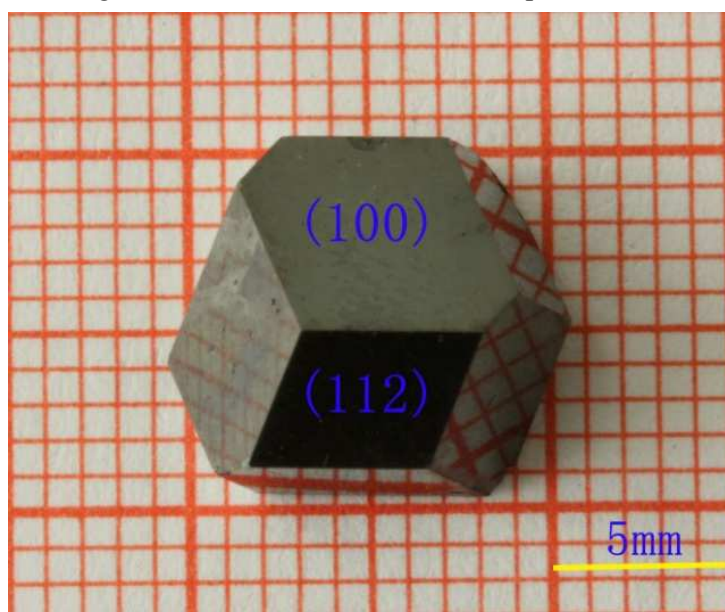
Yangyang Dang,<sup>a</sup> Xutang Tao,<sup>ab\*</sup> Yang Liu,<sup>a</sup> Youxuan Sun,<sup>a</sup> Dongsheng Yuan,<sup>a</sup> Xiaolong Liu,<sup>a</sup> Weiqun Lu,<sup>a</sup> Guangfeng Liu,<sup>a</sup> Haibing Xia<sup>a\*</sup>

<sup>a</sup> State Key Laboratory of Crystal Materials, Shandong University, No.27 Shanda South Road, Jinan, 250100, China.

<sup>b</sup> Key Laboratory of Functional Crystal Materials and Device (Shandong University, Ministry of Education), No.27 South Shanda Road, Jinan, 250100, China

E-mail: txt@sdu.edu.cn; Fax: +86-531-88574135; Tel: +86-531-88364963; E-mail: hbxia@sdu.edu.cn.

Bulk crystal of tetragonal  $\text{CH}_3\text{NH}_3\text{PbI}_3$  with dimensions to centimeters grown by temperature-lowering method in HI solution was first reported.



## ARTICLE

# Bulk Crystal Growth of Hybrid Perovskite Material $\text{CH}_3\text{NH}_3\text{PbI}_3$ †

Cite this: DOI: 10.1039/x0xx00000x

Yangyang Dang,<sup>a</sup> Xutang Tao,<sup>ab\*</sup> Yang Liu,<sup>a</sup> Youxuan Sun,<sup>a</sup> Dongsheng Yuan,<sup>a</sup> Xiaolong Liu,<sup>a</sup> Weiqun Lu,<sup>a</sup> Guangfeng Liu,<sup>a</sup> Haibing Xia,<sup>a\*</sup>Received 00th January 2012,  
Accepted 00th January 2012

DOI: 10.1039/x0xx00000x

[www.rsc.org/](http://www.rsc.org/)

The organic-inorganic hybrid perovskite materials have received numerous focuses due to their promising applications in many optoelectronic fields. However, some of the fundamental properties of perovskite materials are still disputable, because most of them are derived from thin-film state. To comprehend the intrinsic characteristics in single crystal, here we report, for the first time, the bulk crystal growth of  $\text{CH}_3\text{NH}_3\text{PbI}_3$ . The single crystals of tetragonal  $\text{CH}_3\text{NH}_3\text{PbI}_3$  with dimensions of 10 mm × 10 mm × 8 mm were grown by temperature-lowering method in HI solution. The refinement and orientations of  $\text{CH}_3\text{NH}_3\text{PbI}_3$  single crystal structure are conducted based on a high quality crystal. The absorption edge of  $\text{CH}_3\text{NH}_3\text{PbI}_3$  single crystal locates at about 836 nm. This indicates that the band gap of  $\text{CH}_3\text{NH}_3\text{PbI}_3$  is approximately 1.48 eV, which is closing to the theoretical results and smaller than those derived from polycrystalline and thin-films.  $\text{CH}_3\text{NH}_3\text{PbI}_3$  crystal exhibits a relatively wide absorption (from 250 nm to 800 nm) and relatively good thermal stability.

## Introduction

The main group element halometallates, especially, lead halometallates, are a new class of semiconducting materials, which displayed special photoconductivity,<sup>1</sup> ionic-conductivity,<sup>2</sup> electrical-conductivity,<sup>3, 4, 5</sup> photo-<sup>6</sup> and electroluminescence,<sup>7</sup> exciton formation<sup>8, 9</sup> properties and they have been extensively studied for the applications in the field covered from thin film transistors (TFTs)<sup>10</sup> to solar energy conversion.<sup>11</sup> In the lead halometallates, lead iodometalates with unique properties adopted perovskite type structure with composition of  $\text{APbI}_3$  (A = Rb, Cs or organic cation).<sup>20</sup> The stoichiometry of the material and the lead-iodide connectivity were extremely sensitive to the nature of the cation with both atomic radius and versatility playing a vital role. The  $\{\text{PbI}_6\}$  octahedra existed in the structure of  $\text{APbI}_3$  were affected by the corner-sharing, edge-sharing, and face-sharing forms.<sup>12</sup> The band gap of  $\text{APbI}_3$  semiconductors was easily monitored by modifying either the structure of the inorganic framework or the size of the organic cation.

In the past five years, the methyl-ammonium lead halide, especially  $\text{CH}_3\text{NH}_3\text{PbI}_3$  (MAPbI<sub>3</sub>), has generated significant interests in electronic and photonic applications with special properties.<sup>[11d]</sup> While, recent reports<sup>13-18</sup> for MAPbI<sub>3</sub> were mostly based on the hybrid lead halide perovskite thin film. Many problems remain to be presented regarding the stability

of perovskite thin film and the mechanism for photoelectric conversion. Besides, the report on the carrier mobility of MAPbI<sub>3</sub> polycrystalline or thin film has existed in disputes.<sup>19, 20</sup> The fundamental properties, upon which the performance of single crystal is based, are currently under-explored, making their elucidation a vital issue. To date, there are only three reports on MAPbI<sub>3</sub> single crystal,<sup>20-22</sup> however, none of them are devoted to bulk single crystal growth or the crystal orientations. In this paper, we report the synthesis, bulk crystal growth by temperature-lowering method and the properties of the tetragonal MAPbI<sub>3</sub>. The refinement and orientations of the tetragonal MAPbI<sub>3</sub> single crystal structure are conducted. The experimental results indicated that the absorption edge of the tetragonal MAPbI<sub>3</sub> in the UV-vis spectrum is at 836 nm, and the band gap is approximately 1.48 eV. It exhibits a relatively wide absorption window (from 250 nm to 800 nm), and relatively good thermal stability. These behaviours make the MAPbI<sub>3</sub> single crystal a promising candidate for optical and electronic applications.

## Experimental section

### Reagents

All starting materials were analytical grade from commercial sources.  $\text{CH}_3\text{NH}_2$  solution,  $\text{Pb}(\text{CH}_3\text{COOH})_2 \cdot 3\text{H}_2\text{O}$  and HI

solution were purchased from Sino-pharm and used without further treatment.

### Synthesis of $\text{CH}_3\text{NH}_3\text{I}$

Methylamine  $\text{CH}_3\text{NH}_2$  solution with slight excess was reacted with hydroiodic acid (HI) at ice bath in ambient atmosphere. Crystallization of methyl-ammonium iodide ( $\text{CH}_3\text{NH}_3\text{I}$ ) was achieved using a rotary evaporator. A white colorless microcrystal  $\text{CH}_3\text{NH}_3\text{I}$  was washed and formed with absolute diethyl ether several times, and finally dried at 60 °C in a vacuum oven for overnight (see Fig. S1, ESI†). And the white with yellow microcrystal  $\text{CH}_3\text{NH}_3\text{I}$  was washed and formed with absolute ethanol and then absolute diethyl ether several times, and finally dried at 60 °C in a vacuum oven for overnight (see Fig. S2, ESI†).

### Crystal growth of $\text{CH}_3\text{NH}_3\text{PbI}_3$

The newly synthesized methyl-ammonium iodide ( $\text{CH}_3\text{NH}_3\text{I}$ ) was reacted with  $\text{Pb}(\text{CH}_3\text{COOH})_2 \cdot 3\text{H}_2\text{O}$  in hydroiodic acid (HI) solution in air. A 500 ml round bottom flask was charged with a mixture of the aqueous HI (260 ml). According to the stoichiometric ratio of  $\text{Pb}(\text{CH}_3\text{COOH})_2 \cdot 3\text{H}_2\text{O}$  (37.933g, 0.1 mol) and  $\text{CH}_3\text{NH}_3\text{I}$  (15.9g, 0.1 mol),  $\text{Pb}(\text{CH}_3\text{COOH})_2 \cdot 3\text{H}_2\text{O}$  was dissolved in the aqueous HI, under the constant stirring, forming a yellow solution. And then  $\text{CH}_3\text{NH}_3\text{I}$  was added into the yellow solution. With the decreasing of the solution temperature from 65 to 40 °C to induce the saturation of the solute, the black and shiny crystal of  $\text{CH}_3\text{NH}_3\text{PbI}_3$  with the size of 10 mm × 10 mm × 8 mm was successfully grown in the bottom of the flask after several days and was washed and filtered with HI and then acetone (see Fig. 1). Below 40 °C, the yellow needle-like crystals ( $\text{CH}_3\text{NH}_3$ )<sub>4</sub> $\text{PbI}_6 \cdot 2\text{H}_2\text{O}$ <sup>21, 23</sup> appeared at the bottom of the flask.

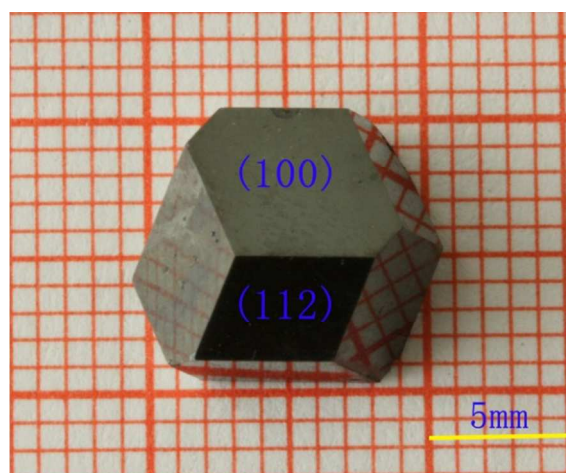


Fig.1 The photograph of  $\text{CH}_3\text{NH}_3\text{PbI}_3$  oriented to exhibited natural facets {100} and {112}

### Single-crystal structure determination

Single crystal of tetragonal  $\text{MAPbI}_3$  with dimensions of ca.  $0.07 \times 0.06 \times 0.05 \text{ mm}^3$  was selected and used for the single-

crystal diffraction experiment. Data sets of tetragonal  $\text{MAPbI}_3$  were collected using a Bruker SMART APEX-II diffractometer equipped with a CCD detector (graphite-monochromated  $\text{Mo-K}\alpha$  radiation,  $\lambda = 0.71073 \text{ \AA}$ ) at 293(2) K. Data integration and cell refinement were performed using the *APEX2* software.<sup>24</sup> The structure was solved by direct methods and refined using the *SHELXTL* 97 software package.<sup>24</sup> All of non-hydrogen atoms of the structure were refined with anisotropic thermal parameters, and the refinements converged for  $F_o^{2>} > 2\sigma(F_o^2)$ . All the calculations were performed using *SHELXTL* crystallographic software package.<sup>24</sup> Symmetry analysis on the model using *PLATON*<sup>25</sup> revealed that no obvious space group change was needed. In the refinement, the commands *EDAP* and *EXYZ* were used to restrain some related bond lengths and bond angles.

### Powder X-ray diffraction and $^1\text{H}$ and $^{13}\text{C}$ NMR spectroscopy

X-Ray powder diffraction (XRD) patterns of polycrystalline material were collected using a Bruker-AXS D8 ADVANCE X-Ray diffractometer with  $\text{Cu-K}\alpha 1$  radiation ( $\lambda = 1.54186 \text{ \AA}$ ) in the range of  $10^\circ$ - $90^\circ$  ( $2\theta$ ) with a step size of  $0.002^\circ$  and time setting of 0.1 s per step. No impurity peaks were observed. The powder XRD patterns for MAI and  $\text{MAPbI}_3$  obtained from solution reaction are in good agreement with the calculated XRD patterns from the single-crystal models in Fig. S3 and Fig. 4, respectively. The  $^1\text{H}$  and  $^{13}\text{C}$  Nuclear Magnetic Resonance (NMR) spectra were recorded in dimethyl sulfoxide (DMSO) using a Bruker Advance 300 spectrometers.

### UV-vis diffuse reflectance spectrum

UV-Vis diffuse reflectance spectroscopy was performed on a Shimadzu UV 2550 spectrophotometer equipped with an integrating sphere over the spectral range 200–900 nm. A  $\text{BaSO}_4$  plate was used as the standard (100% reflectance), on which the finely ground sample from the crystal was coated. The absorption spectrum was calculated from the reflectance spectrum using the Kubelka–Munk function:  $\alpha/S = (1-R)^2/(2R)$ ,<sup>26</sup> where  $\alpha$  is the absorption coefficient,  $S$  is the scattering coefficient, and  $R$  is the reflectance.

### Thermogravimetric analysis (TGA)

Differential scanning calorimetry (DSC) and thermogravimetric analysis (TGA) were carried out on a TGA/DSC1/1600HT analyzer (METTLER TOLEDO Instruments). The sample was placed in  $\text{Al}_2\text{O}_3$  crucible, and heated at a rate of  $10^\circ \text{C min}^{-1}$  from room temperature to 800 °C under flowing nitrogen gas.

## Result and discussion

### Synthesis, Solubility and Crystal growth

The MAI was synthesized via a reaction of slight excess of  $\text{CH}_3\text{NH}_2$  solution and hydroiodic acid (HI) in ambient atmosphere. The  $^1\text{H}$  and  $^{13}\text{C}$  nuclear magnetic resonance (NMR) of the white powder were characterized to verify the identity and purity of the MAI, where no presence of any

impurity was found (see Figure S4-5, ESI†). Below 40 °C, the yellow needle-like crystals  $\text{MA}_4\text{PbI}_6 \cdot 2\text{H}_2\text{O}^{21, 23}$  were formed, and gradually decomposed to light yellow  $\text{PbI}_2$  when exposed to the air two or three days. Besides,  $\text{MA}_4\text{PbI}_6 \cdot 2\text{H}_2\text{O}$  decomposed and changed into black  $\text{MAPbI}_3$  promptly when heated to above 50°C. The solubility curve of  $\text{MAPbI}_3$  in HI solution is shown in Figure 2. The crystal growths were performed in an alternative temperature water bath of controlled stability (0.1 °C). Solutions were prepared using HI solution as a solvent and saturated at 65 °C. They were preheated to 70 °C for 24 h in a sample holder. This procedure was performed to ensure that all ingredients were dissolved. With the decreasing of the solution temperature from 65 to 40 °C to induce the saturation of the solute, bulk single crystals of  $\text{MAPbI}_3$  were grown in the solution after a growth period of about one month. The size of the single crystal reached  $10\text{mm} \times 10\text{mm} \times 8\text{mm}$  (see Fig. 1).

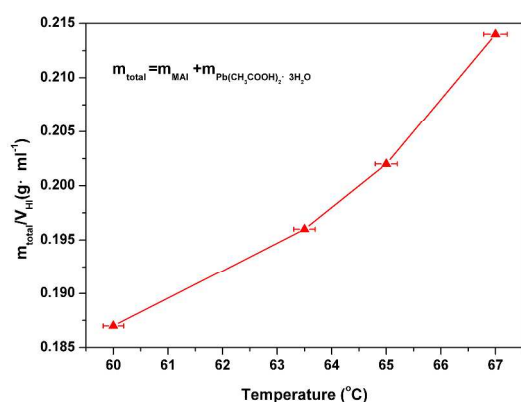


Fig.2 Solubility curve of  $\text{CH}_3\text{NH}_3\text{PbI}_3$  in HI solution

### Crystal structure

The exhibited natural facets were determined to be hexagon  $\{100\}$  and parallelogram  $\{112\}$  using X-ray diffraction (see Fig. 1). Crystallographic analysis reveals that the crystal structure of  $\text{MAPbI}_3$  belongs to the tetragonal system with space group  $I4cm$  (No.108) at room temperature. Single crystal X-ray diffraction data and selected bond lengths and bond angles for  $\text{MAPbI}_3$  are presented in Table 1 and 2. The related isotropic and anisotropic displacement parameters are displayed in Table S2 and S3 (see ESI†). However, the report about  $\text{MAPbI}_3$  has displayed a distorted three-dimensional perovskite structure that crystallized in the tetragonal  $I4/mcm$  (No.140) space group as schematically illustrated in 1987.<sup>27</sup> Moreover, in the ref. 20, all the non-hydrogen atoms were refined without extinction coefficient parameters, and X-ray diffraction easily distinguished between C and N based on the sample with dimensions of ca.  $0.005 \times 0.003 \times 0.002 \text{ mm}^3$ . In our current results, the crystal structure of  $\text{MAPbI}_3$  was re-determined and refined by single crystal diffraction. The lattice parameters are larger and the bond lengths of  $\text{MAPbI}_3$  are

shorter than those earlier reported<sup>20</sup> (see Table S1, ESI†). The Polyhedral diagrams of  $\text{MAPbI}_3$  crystal are shown in Fig.3. In the crystal structure of  $\text{MAPbI}_3$ , the  $\{\text{PbI}_6\}$  octahedral structure unit existed in the distortion along the  $\{001\}$  direction and with symmetry along other directions. Probably alternate C/N atoms, in the C-N structure unit exist in the presence of disorder phenomena so that the distribution of C and N is at random in the C-N bond position. It is this special bond arrangement that makes the  $\text{MAPbI}_3$  show the asymmetric structure.

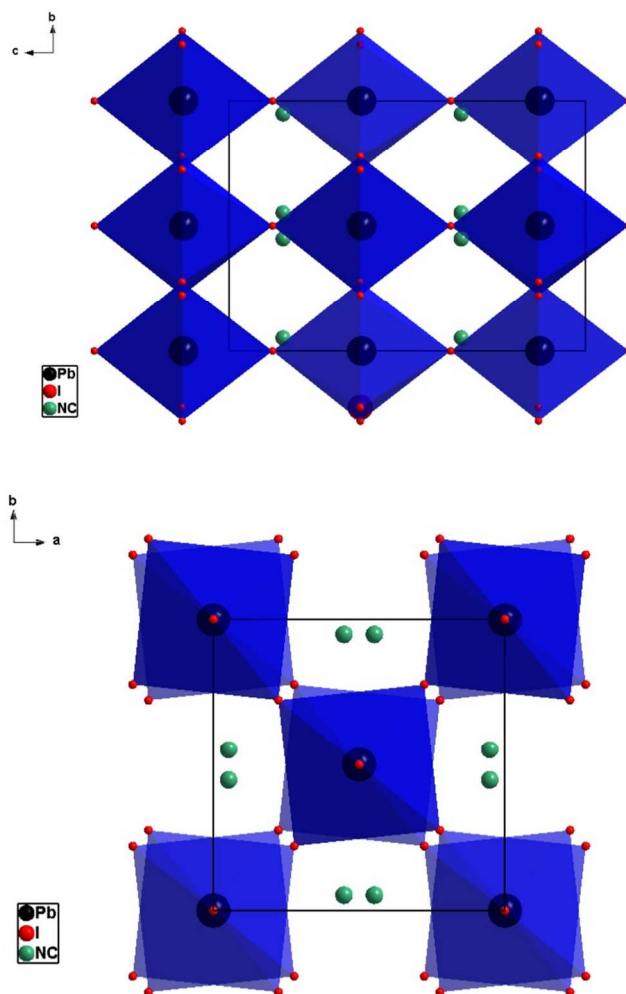


Fig.3 Polyhedral representation of  $\text{MAPbI}_3$  crystal structure along the  $\{100\}$  and  $\{001\}$  directions.

Table 1 Crystal data and structure refinement for MAPbI<sub>3</sub>

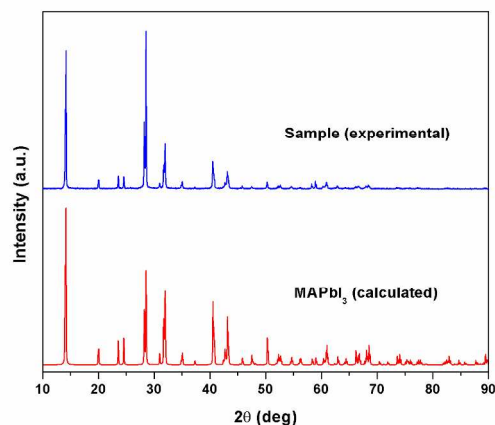
Empirical formula	MAPbI <sub>3</sub>
Formula weight/g mol <sup>-1</sup>	619.96
Temperature/K	293(2)
Crystal color	black
Wavelength/Å	0.71073
Crystal system	Tetragonal
Space group	I4cm (No.108)
a/Å	8.896(3)
b/Å	8.896(3)
c/Å	12.637(4)
α/°	90
β/°	90
γ/°	90
Volume/Å <sup>3</sup>	1000.0(6)
Z	4
Density/g cm <sup>-3</sup>	4.118
μ(mm <sup>-1</sup> )	26.049
Absolute structure Flack parameter	0.44(7)
F(000)	1040
Crystal size (mm <sup>3</sup> )	0.07×0.06×0.05
Theta range (data collection)	3.22 to 27.64 °
Limiting indices	-11<=h<=11, -11<=k<=11, -16<=l<=16
Reflections collected / unique	5293 / 631 [R(int) = 0.0569]
Completeness to theta = 27.64	99.7 %
GOF on F <sup>2</sup>	1.223
Absorption correction	Semi-empirical from equivalents
Data / restraints / parameters	631 / 1 / 20
R1, wR1 [I > 2σ(I)]	0.0644/0.1468
R2, wR2 (all data)	0.0710/0.1494
Extinction coefficient	0.0024(2)
Min/Max Δρ/eÅ <sup>-3</sup>	-4.065/3.531
w=1/[σ <sup>2</sup> (Fo <sup>2</sup> )+(0.0636P) <sup>2</sup> +0.0000P] where P=(Fo <sup>2</sup> +2Fc <sup>2</sup> )/3	

Table 2 Selected bond lengths(Å) and bond angles(deg) for MAPbI<sub>3</sub>

Pb(01)-I(002)	3.159(11)
Pb(01)-I(002)#1	3.159(11)
Pb(01)-I(003)	3.1637(11)
Pb(01)-I(003)#2	3.1637(11)
Pb(01)-I(003)#3	3.1637(11)
Pb(01)-I(003)#4	3.1637(11)
I(002)-Pb(01)#5	3.159(11)
I(003)-Pb(01)#6	3.1637(11)
N(1)-C(1)#7	1.32(10)
I(002)-Pb(01)-I(002)#1	180.0
I(002)-Pb(01)-I(003)	90.83(19)
I(002)#1-Pb(01)-I(003)	89.17(19)
I(002)-Pb(01)-I(003)#2	90.83(19)
I(002)#1-Pb(01)-I(003)#2	89.17(19)
I(003)-Pb(01)-I(003)#2	178.3(4)
I(002)-Pb(01)-I(003)#3	90.83(19)
I(002)#1-Pb(01)-I(003)#3	89.17(19)
I(003)-Pb(01)-I(003)#3	89.988(6)
I(003)#2-Pb(01)-I(003)#3	89.988(6)
I(002)-Pb(01)-I(003)#4	178.3(4)
Pb(01)#6-I(003)-Pb(01)	167.60(15)

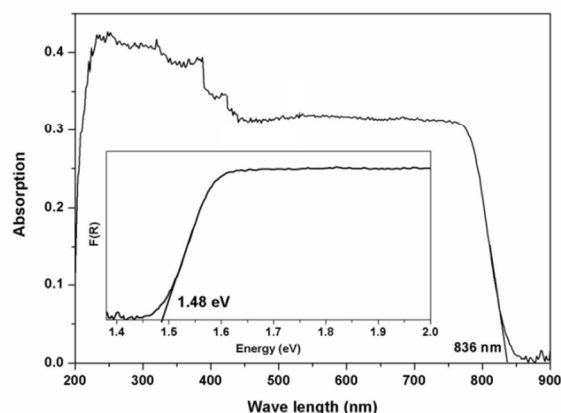
Symmetry transformations used to generate equivalent atoms:

- #1 -x, y, z+1/2 #2 -x, -y, z #3 y, -x, z  
 #4 -y, x, z #5 -x, y, z-1/2 #6 -x+1/2, y+1/2, z+0  
 #7 -x+1, -y+2, z

Fig.4 Calculated and experimental powder X-ray diffraction patterns for MAPbI<sub>3</sub>.

### Optical property

The UV-vis diffuse reflectance spectrum for MAPbI<sub>3</sub> is shown in Fig. 5. The result of the band structure calculation implies that tetragonal MAPbI<sub>3</sub> has a direct band gap,<sup>28, 29</sup> The band gap can be determined by fixing the tangent line of the curve and the (*hν*) axis. MAPbI<sub>3</sub> is black, and the UV-vis spectrum shows that the absorption edge is at about 836 nm for MAPbI<sub>3</sub>. This indicates that a band gap of CH<sub>3</sub>NH<sub>3</sub>PbI<sub>3</sub> is approximately 1.48 eV, which is closing to the theoretical results<sup>30</sup> and smaller than those derived from polycrystalline and thin-films.<sup>11a, 20, 31</sup> Based on this data, this implies that MAPbI<sub>3</sub> exhibits a relatively narrow band gap semiconductor. It exhibits a relatively wide absorption (from 250 nm to 800 nm) all over the UV-vis spectrum.

Fig.5 UV-vis diffuse reflectance spectroscopy plots for MAPbI<sub>3</sub>

### Thermogravimetric analysis and Stability

The TG curve reveals that MAPbI<sub>3</sub> is thermally stable up to 300 °C when it starts losing weight (Figure 6). From 300 °C to 500 °C, the compound continues to lose weight until about 70% left. This implies that the residue is mainly light yellow PbI<sub>2</sub> (see

Fig. S6, ESI†), which is consistent with the report.<sup>[32]</sup> The black and shiny crystal MAPbI<sub>3</sub> is not hygroscopic and has relatively good stability after being exposed to air several days. Besides, the stability of newly made MAPbI<sub>3</sub> single crystal in four different solvents (distilled water, ethanol, acetone and ethyl acetate) was also tested. The experiment showed that MAPbI<sub>3</sub> single crystal was stable in acetone and ethyl acetate, but promptly decomposed to light yellow PbI<sub>2</sub> in distilled water and ethanol.

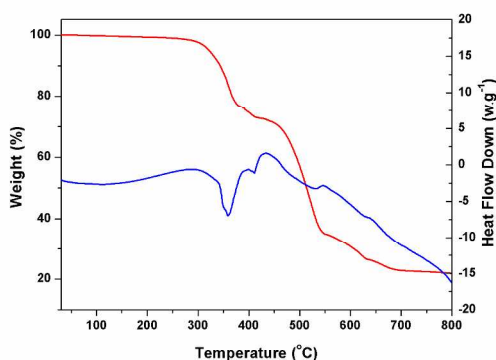


Fig.6 TGA and DSC data for MAPbI<sub>3</sub>

## Conclusions

In conclusion, bulk crystal growth of MAPbI<sub>3</sub> by temperature-lowering method was first reported, which resulted from a reaction of CH<sub>3</sub>NH<sub>3</sub>I and Pb(CH<sub>3</sub>COOH)<sub>2</sub>·3H<sub>2</sub>O in HI solution. And the refinement and orientations of MAPbI<sub>3</sub> single crystal structure are conducted. It is covered with all the UV-vis spectrum and relatively good thermal stability. Besides, its band gap is approximately 1.48 eV, which indicates a relatively narrow band gap semiconductor. These behaviours make the MAPbI<sub>3</sub> single crystal a promising candidate for optical and electronic applications. The further study of other properties for MAPbI<sub>3</sub> single crystal is under way.

## Acknowledgements

We thank the National Natural Science Foundation of China (grant no. 51321091, 51227002, 51272129) and the Program of Introducing Talents of Disciplines to Universities in China (111 program no. b06015).

## Notes and references

<sup>a</sup> State Key Laboratory of Crystal Materials, Shandong University, No. 27 Shanda South Road, Jinan, 250100, China.

<sup>b</sup> Key Laboratory of Functional Crystal Materials and Device (Shandong University, Ministry of Education), No. 27 South Shanda Road, Jinan, 250100, China.

E-mail: [txt@sdu.edu.cn](mailto:txt@sdu.edu.cn); Fax: +86-531-88574135; Tel: +86-531-88364963; E-mail: [hbxia@sdu.edu.cn](mailto:hbxia@sdu.edu.cn).

Electronic Supplementary Information (ESI) available: [CCDC 1029776; the photographs of white MAI, white with yellow MAI and residue light yellow PbI<sub>2</sub>; powder X-ray diffraction patterns for MAI; <sup>1</sup>H-NMR and <sup>13</sup>C-NMR spectra of MAI; Selected bond length(Å) and bond angles(deg) for β-MAPbI<sub>3</sub>]. See DOI: 10.1039/b000000x/

1. C. K. Moller, *Nature*, 1958, **182**, 1436.
2. J. Mizusaki, K. Arai, K. Fueki, *Solid State Ionics*, 1983, **11**, 203.
3. D. B. Mitzi, C. A. Feild, W. T. A. Harrison, A. M. Guloy, *Nature*, 1994, **369**, 467.
4. D. B. Mitzi, S. Wang, C. A. Feild, C. A. Chess, A. M. Guloy, *Science*, 1995, **267**, 1473.
5. I. Chung, J. -H. Song, J. Im, J. Androulakis, C. D. Malliakas, H. Li, A. J. Freeman, J. T. Kenney, M. G. Kanatzidis, *J. Am. Chem. Soc.*, 2012, **134**, 8579.
6. D. B. Mitzi, *Chem. Mater.*, 1996, **8**, 791.
7. K. Chondroudis, D. B. Mitzi, *Chem. Mater.*, 1999, **11**, 3028.
8. J. Calabrese, N. L. Jones, R. L. Harlow, N. Herron, D. L. Thorn, Y. Wang, *J. Am. Chem. Soc.*, 1991, **113**, 2328.
9. K. Tanaka, T. Takahashi, T. Ban, T. Kondo, K. Uchida, N. Miura, *Solid State Commun.*, 2003, **127**, 619.
10. C. R. Kagan, D. B. Mitzi, C. D. Dimitrakopoulos, *Science*, 1999, **286**, 945.
11. (a) A. Kojima, K. Teshima, Y. Shirai, T. Miyasaka, *J. Am. Chem. Soc.*, 2009, **131**, 6050. (b) I. Chung, B. Lee, J. He, R. P. H. Chang, M. G. Kanatzidis, *Nature*, 2012, **485**, 486. (c) M. M. Lee, J. Teuscher, T. Miyasaka, T. N. Murakami, H. J. Snaith, *Science*, 2012, **338**, 643. (d) Philip Schulz, Eran Edri, Saar Kirmayer, Gary Hodes, David Cahen and Antoine Kahn, *Energy Environ. Sci.*, 2014, **7**, 1377. (e) H. Zhou, Q. Chen, G. Li, S. Luo, T. Song, H. Duan, Z. Hong, J. You, Y. Liu, Y. Yang, *Science*, 2014, **345**, 542. (f) Y. Yamada, T. Nakamura, M. Endo, A. Wakamiya, and Y. Kanemitsu, *J. Am. Chem. Soc.*, 2014, **133**, 11610. (g) Jun Hong Noh, Sang Hyuk Im, Jin Hyuck Heo, Tarak N. Mandal, and Sang Il Seok, *Nano Lett.*, 2013, **13**, 1764. (h) L. Wang, C. Mc Cleese, A. Kovalsky, Y. Zhao and C. Burda, *J. Am. Chem. Soc.*, 2014, **136**, 12205.
12. (a) Z. Tang, A. M. Guloy, *J. Am. Chem. Soc.*, 1998, **121**, 452. (b) H.-R. Zhao, D.-P. Li, X.-M. Ren, Y. Song, W.-Q. Jin, *J. Am. Chem. Soc.*, 2009, **132**, 18.
13. Emilio J. Juarez-Perez, Michael Wußler, Francisco Fabregat-Santiago, Kerstin Lakus-Wollny, Eric Mankel, Thomas Mayer, Wolfram Jaegermann, and Ivan Mora-Sero, *J. Phys. Chem. Lett.*, 2014, **5**, 680.
14. Jeffrey A. Christians, Raymond C. M. Fung, Prashant V. Kamat, *J. Am. Chem. Soc.*, 2014, **136**, 758.
15. Q. Chen, H. Zhou, Z. Hong, S. Luo, H. Duan, H. Wang, Y. Liu, G. Li, and Y. Yang, *J. Am. Chem. Soc.*, 2014, **136**, 622.
16. Y. Zhao, A. M. Nardes, and Kai Zhu, *J. Phys. Chem. Lett.*, 2014, **5**, 490.
17. C. N. Hoth, S. A. Choulis, P. Schilinsky and C. J. Brabec, *Adv. Mater.*, 2007, **19**, 3973.
18. Julian Burschka, Norman Pellet, Soo-Jin Moon, Robin Humphry-Baker, Peng Gao, Mohammad K. Nazeeruddin, Michael Graetzel, *Nature*, 2013, **499**, 316.
19. Hikaru Oga, Akinori Saeki, Yuhei Ogomi, Shuzi Hayase, and Shu Seki, *J. Am. Chem. Soc.*, 2014, **136**, 13818.

## ARTICLE

20. C. C. Stoumpos, C. D. Malliakas, and M. G. Kanatzidis, *Inorg. Chem.*, 2013, **52**, 9019.
21. T. Baikie, Y. Fang, J. M. Kadro, M. Schreyer, F. Wei, S. G. Mhaisalkar, Michael Graetzel and T. J. White, *J. Mater. Chem. A*, 2013, **1**, 5628.
22. Andrea Pisoni, Jacim Jacimovic, Osor S. Barisic, Massimo Spina, Richard Gaa, La'szlo Forro, and Endre Horvath, *J. Phys. Chem. Lett.*, 2014, **5**, 2488.
23. B. R. Vincent, K. N. Robertson, T. S. Cameron and K. Osvald, *Can. J. Chem.*, 1987, **65**, 1042.
24. Bruker. APEX2, Bruker Analytical X-ray Instruments, Inc., Madison, Wisconsin, USA., 2005.
25. G. M. Sheldrick, Bruker Analytical X-ray Instruments, Inc., Madison, WI, 2001.
26. A. L. Spek, *J. Appl. Crystallogr.*, 2003, **36**, 7.
27. A. Poglitsch and D. Weber, *J. Chem. Phys.*, 1987, **87**, 6373.
28. P. Kubelka and F. Z. Munk, *Tech. Physik.*, 1931, **12**, 593.
29. Y. Zhao and K. Zhu, *J. Phys. Chem. Lett.*, 2013, **4**, 2880.
30. H. S. Kim, C. R. Lee, J. H. Im, K. B. Lee, T. Moehl, A. Marchioro, S. J. Moon, R. Humphry-Baker, J. H. Yum, J. E. Moser, M. Graetzel and N. G. Park, *Sci. Rep.*, 2012, **2**, 591.
31. Stefaan De Wolf, Jakub Holovsky, Soo-Jin Moon, Philipp Löper, Bjoern Niesen, Martin Ledinsky, Franz-Josef Haug, Jun-Ho Yum, and Christophe Ballif, *J. Phys. Chem. Lett.*, 2014, **5**, 1035.
32. R. J. M. Konings, A. Kok-Scheele, and E. H. P. Cordfunke, *Thermochim. Acta*, 1995, **261**, 221.